Protamine is an antagonist of apelin receptor, and its activity is reversed by heparin

Sophie Le Gonidec,[*,†,1] Carline Chaves-Almagro,[*,1] Yushi Bai,[‡] Hye Jin Kang,[§] Allyson Smith,[‡] Estelle Wanecq,[*] Xi-Ping Huang,[§] Hervé Prats,[¶] Bernard Knibiehler,[¶] Bryan L. Roth,[§] Larry S. Barak,[‡] Marc G. Caron,[‡,‖,#] Philippe Valet,[*] Yves Audigier,[*] and Bernard Masri[*,2]

[*]Institut des Maladies Métaboliques et Cardiovasculaires, INSERM Unité 1048, [†]Service Phénotypage, Centre Régional d'Exploration Fonctionnelle et Ressources Expérimentales, INSERM US006, and [¶]Centre de Recherches en Cancérologie de Toulouse, Unités Mixte de Recherche 1037 INSERM, Université de Toulouse, Université Paul Sabatier, Toulouse, France; [‡]Department of Cell Biology, [‖]Department of Medicine, and [#]Department of Neurobiology, Duke University Medical Center, Durham, North Carolina, USA; and [§]Department of Pharmacology, University of North Carolina at Chapel Hill Medical School, Chapel Hill, North Carolina, USA

ABSTRACT: Apelin signaling plays an important role during embryo development and regulates angiogenesis, cardiovascular activity, and energy metabolism in adulthood. Overexpression and hyperactivity of this signaling pathway is observed in various pathologic states, such as cardiovascular diseases and cancer, which highlights the importance of inhibiting apelin receptor (APJ); therefore, we developed a cell-based screening assay that uses fluorescence microscopy to identify APJ antagonists. This approach led us to identify the U.S. Food and Drug Administration–approved compound protamine—already used clinically after cardiac surgery—as an agent to bind to heparin and thereby reverse its anticlotting activity. Protamine displays a 390-nM affinity for APJ and behaves as a full antagonist with regard to G protein and β-arrestin–dependent intracellular signaling. *Ex vivo* and *in vivo*, protamine abolishes well-known apelin effects, such as angiogenesis, glucose tolerance, and vasodilatation. Remarkably, protamine antagonist activity is fully reversed by heparin treatment both *in vitro* and *in vivo*. Thus, our results demonstrate a new pharmacologic property of protamine—blockade of APJ—that could explain some adverse effects observed in protamine-treated patients. Moreover, our data reveal that the established anti-angiogenic activity of protamine would rely on APJ antagonism.—Le Gonidec, S., Chaves-Almagro, C., Bai, Y., Kang, H. J., Smith, A., Wanecq, E., Huang, X.-P., Prats, H., Knibiehler, B., Roth, B. L., Barak, L. S., Caron, M. G., Valet, P., Audigier, Y., Masri, B. Protamine is an antagonist of apelin receptor, and its activity is reversed by heparin. FASEB J. 31, 2507–2519 (2017). www.fasebj.org

KEY WORDS: GPCR · APJ · angiogenesis · metabolism · blood pressure

Apelin signaling is involved in a wide range of physiologic functions, participating in regulation of cardiovascular and body fluid homeostasis, as well as in the control of energy metabolism (1). Apelin receptor, also named APJ [putative receptor protein related to the angiotensin II type 1a receptor (AT1aR)], is a class A GPCR, which shares 31% sequence identity with AT1aR (2). Its endogenous ligand, apelin, is a prepropeptide of 77 aa, which gives rise, after proteolytic cleavage, to apelin 36, apelin 17, apelin 13, and the pyroglutaminated form pyro-apelin 13 (3, 4). All apelin fragments inhibit forskolin-induced cAMP production (5, 6); activate different intracellular effectors, such as ERKs, PI3K/Akt, and AMPK; and trigger β-arrestin recruitment to APJ (7–10), thereby promoting cell metabolism, survival, proliferation, and migration. Recently, a second endogenous peptide ligand of APJ, named Elabela/Toddler, has been identified and observed to play a crucial role in normal heart and vasculature development during embryogenesis (11, 12).

Whereas Elabela/Toddler is mainly expressed in human embryonic stem cells and in the adult kidney and prostate (13, 14), apelin and its receptor are widely expressed in mammalian organisms (15). They are also expressed in various brain regions that are known to regulate food

ABBREVIATIONS: APJ, apelin receptor; AT1aR, angiotensin II type 1a receptor; BRET, bioluminescence resonance energy transfer; CAM, chicken embryo chorioallantoic membrane; CXCR4, C-X-C chemokine receptor type 4; FCS, fetal calf serum; FDA, U.S. Food and Drug Administration; GFP, green fluorescent protein; HA, hemagglutinin; hAPJ, human apelin receptor; Rluc, *Renilla* luciferase; TAMRA, 5-carboxytetramethylrhodamine; VEGF, vascular endothelial growth factor; YFP, yellow fluorescent protein

[1] These authors contributed equally to this work.

[2] Correspondence: Institut des Maladies Métaboliques et Cardiovasculaires, INSERM U1048, Université de Toulouse, UPS, Toulouse III, CHU Rangueil, Bât L4, 1, Avenue Jean Poulhès - BP 84225, 31432 Toulouse, France. E-mail: bernard.masri@inserm.fr

doi: 10.1096/fj.201601074R

This article includes supplemental data. Please visit *http://www.fasebj.org* to obtain this information.

intake, glucose, and fluid homeostasis, the highest expression detected in hypothalamic nuclei (16, 17). Moreover, apelin possesses neuroprotective effects in the CNS (18, 19). At the peripheral level, apelin's effects on energy metabolism have been extensively described (20). In particular, apelin infusion improves glucose tolerance and decreases glycemia by stimulating glucose uptake in skeletal muscle and adipose tissue, thereby improving insulin sensitivity (8, 21).

In the cardiovascular system, apelin acts as a potent inotropic agent and reduces cardiac loading (22). Moreover, intravenous infusion of apelin in humans induces an NO-dependent arterial vasodilatation (23), which reduces mean arterial blood pressure. Of interest, this effect is abolished in APJ–deficient mice (24). In addition, apelin displays all the properties of an angiogenic factor by promoting proliferation and migration of endothelial cells (10, 25).

In addition to its physiologic functions, apelin signaling is also associated with cardiovascular and metabolic diseases, such as atherosclerosis (26, 27), hypertension (28), and type 2 diabetes (29). Furthermore, overexpression and hyperactivity of apelin signaling are linked with different pathologic states that promote neoangiogenesis. Indeed, in the retina, apelin transcripts and proteins are significantly increased during development of retinal vascular diseases and diabetic retinopathy (30, 31). Of note, apelin concentrations in the vitreous of patients strictly parallel proliferative diabetic retinopathy and the extent of vessel proliferation (32). Intravitreal injection of an APJ antagonist—apelin F13A peptide analog—strongly reduces the gene and protein expression of glial fibrillary acidic protein and the angiogenic factor, VEGF, in the retina of diabetic rats (30).

As with many GPCRs (33), expression of APJ and its cognate ligand apelin is also up-regulated in several cancers (34–37). Furthermore, serum and tumor apelin levels positively correlate with tumor progression and poor overall survival (35, 38, 39). Indeed, APJ expression mediates survival and migration of tumor cells (35, 37), whereas apelin expression promotes tumor neoangiogenesis (34, 38, 40), lymphangiogenesis, and lymph node metastasis (41).

Accordingly, APJ antagonists could represent interesting clinical molecules for blocking increased activity of apelin signaling in pathologic angiogenesis.

To date, few compounds with antagonist activity on APJ have been identified (42, 43). We thus developed a fluorescence-based, high-throughput screening and identified the U.S. Food and Drug Administration (FDA)–approved compound, protamine, which is used after cardiac surgery to reverse the anticlotting effect of heparin. By using different biophysical and *in vitro* approaches, we demonstrate that protamine displays a 390-nM affinity for APJ and fully abolishes apelin-induced G-protein activation and β-arrestin recruitment. Similarly, protamine fully inhibits well-described *in vivo* effects of apelin, such as angiogenesis, vasodilatation, and glucose tolerance. Of interest, all these antagonist effects are completely reversed by heparin. Thus, these results clearly demonstrate that protamine inhibits activation of APJ and therefore represents a promising drug to treat diseases that are associated with neoangiogenesis and cancer.

MATERIALS AND METHODS

Reagents

Abs to anti–phospho-p44/42 MAPK (4370, clone D13.14.4E), anti–phospho-S473 Akt (4060, clone D9E), anti-Akt (4691, clone C67E7), and horseradish peroxidase–conjugated secondary Abs were from Cell Signaling Technology (Montigny-le-Bretonneux, France). Abs to anti-ERK2 (sc-154, clone C-14) was from Santa Cruz Biotechnology (Santa Cruz, CA, USA). Pyro-apelin 13 (except as otherwise indicated, pyro-apelin 13 was the only apelin fragment used in the different experiments) and apelin 12 were from Bachem (Bubendorf, Switzerland). Apelin 13-TAMRA (5-carboxytetramethylrhodamine), Elabela 11, Elabela 22, and Elabela 32 were from Proteogenix (Oberhausbergen, France). Angiotensin II was from Sigma-Aldrich (St. Louis, MO, USA). Injectable solutions of protamine sulfate (Protamine Choay; Supplemental Table 1) and heparin sodium (Héparine Choay) were obtained from Sanofi (Paris, France). Coelenterazine *h* was purchased from Promega (Madison, WI, USA) and *Bandeiraea simplicifolia* isolectin B_4 conjugated to FITC, VEGF, and poly-D-lysine hydrobromide were from Sigma-Aldrich. [^{125}I]-Apelin-13 was obtained from Phoenix Pharmaceuticals (Burlingame, CA, USA).

Mice

All procedures were performed in accordance with institutional guidelines for animal research and were approved by the INSERM Animal Care and Use Committee. Male C57Bl/6J mice (15 wk old; for oral glucose tolerance test and *in vivo* blood pressure measurement), and female Balb/c mice (9 wk old; for the tumor growth model) were obtained from Charles River Laboratory (L'Arbresle, France). Mice were conventionally housed in a constant temperature (20–22°C) and humidity (50–60%) animal room, with a 12-h light/dark cycle and free access to food and water.

Cell culture and transfections

HEK293T and U2OS cell lines were purchased from the American Type Culture Collection (Manassas, VA, USA) and cultured in DMEM or minimum essential medium, respectively, supplemented with 10% fetal calf serum (FCS), 2 mM L-glutamine, 100 U/ml penicillin, and 100 μg/ml streptomycin (Thermo Fisher Scientific, Waltham, MA, USA) in a 5% CO_2 humidified incubator at 37°C. All cells were tested for mycoplasma on initial culture by using a Mycoprobe *Mycoplasma* detection kit (CUL001B; R&D Systems, Minneapolis, MN, USA) according to the manufacturer's instructions. No mycoplasma-positive cells were used in this work.

Stable and transient transfections were realized by using a calcium phosphate protocol according to the manufacturer's protocol (Thermo Fisher Scientific).

To generate U2OS cells that stably expressed human APJ (hAPJ) and β-arrestin 2–green fluorescent protein (GFP), U2OS cells were cotransfected with the plasmids pREN-hAPJ and pEGFP-β-arrestin2 and selected to permanently express hAPJ and β-arrestin 2 by using geneticin (400 μg/ml) and zeocin (200 μg/ml). U2OS cells were then kept in culture with 200 μg/ml geneticin and 100 μg/ml zeocin.

For bioluminescence resonance energy transfer (BRET) experiments, HEK293T cells were transiently transfected with pEYFP-β-arrestin 2 and phRluc-hAPJ 1 d after cell seeding as previously described (44). After transfection (24 h), cells were plated in poly-D-lysine–coated 96-well microplates (White OptiPlate; PerkinElmer, Villebon-sur-Yvette, France) at a density of 100,000 cells/well in phenol red–free minimum essential medium

that contained 2% of FCS, 10 mM Hepes, and 2mM of L-glutamine. Cells were then cultured for an additional 24 h before experiments.

cDNA constructs

hAPJ gene fragment was inserted into the pREN expression vector as previously described for murine APJ (9). For BRET experiments, hAPJ was amplified by PCR using pREN-hAPJ as template and a 5′ primer (AAAGGATCCATGGAGGAAG-GTGGTGATTTTG) that contained a *Bam*HI restriction site and a 3′ primer (AAAGGTACCGCGTCAACCACAAGGGTCTCCT-GGC) that contained a *Not*I restriction site. PCR product was cloned into a pcDNA3 vector downstream of 2 hemagglutinin (HA) tags, which generated amino-terminally HA-tagged hAPJ. Expression vector that encoded HA-hAPJ fused to *Renilla* luciferase (Rluc) was generated as follows: the full-length coding region of hAPJ that contained HA tags without a stop codon was amplified by PCR by using specific primers with 5′ and 3′ in-frame restriction enzyme sites of *Xho*I and *Kpn*I, respectively, and subcloned into humanized phRluc N3 vector (PerkinElmer). The vector that encodes β-arrestin 2–yellow fluorescent protein (YFP) has been previously described (44). AT1aR-Rluc construct was kindly provided by Robert J. Lefkowitz (Duke University Medical Center). All constructs were sequenced to check reading frame and integrity.

BRET measurement

For BRET assays, phenol red–free medium was removed from HEK293T cells and replaced by PBS that contained calcium and magnesium.

As previously described (44), the assay was carried out at room temperature and started by adding 10 μl coelenterazine *h* to the well to yield a final concentration of 5 μM. Agonist activity of apelin 13, angiotensin II, and protamine was measured 5 min after addition of the Rluc substrate, and plate reading was performed 5 min after. When the assay was conducted to determine the antagonistic properties of protamine against apelin 13 or angiotensin II, protamine was added 1 min after coelenterazine *h*. Readings started 10 min after addition of Rluc substrate.

BRET signal was determined by calculating the ratio of the light emitted at 515–555 nm over the light emitted at 465–505 nm using a Mithras LB940 instrument (Berthold, Bad Wildbad, Germany) and filters with the appropriate band pass. Net BRET signals were determined by subtracting the BRET signal obtained with cells that only expressed Rluc-tagged hAPJ or Rluc-tagged AT1aR from BRET signals obtained with cells that coexpressed each receptor and YFP-tagged β-arrestin 2. Curves were fitted by using a nonlinear regression and log (agonist or inhibitor) *vs*. response fit equation using GraphPad Prism 5 (GraphPad Software, La Jolla, CA, USA).

For time course analysis of hAPJ-β-arrestin 2 interactions, coelenterazine *h* was added 10 min before reading of samples that were collected at 1-s intervals for 15 min. Protamine was added just before reading. Apelin 13 was injected in the well 200 s later, and heparin was then injected 200 s after apelin 13 by using the Mithras microinjectors that allowed automatic delivery.

Fluorescence microscopy and screening

U2OS cells that stably coexpressed hAPJ and β-arrestin 2-GFP were seeded on poly-D-lysine–coated glass slides in 12-well dishes (3×10^5 cells/well). Twelve hours later, medium was replaced by fresh medium that contained no FCS, and cells were stimulated or not with apelin 13-TAMRA, Elabela 11, Elabela 22, or Elabela 32 for 1 h, then fixed for 15 min in 4% paraformaldehyde in PBS. To determine the antagonist activity of protamine on Elabela fragments, U2OS cells were pretreated with protamine for 10 min, then stimulated with Elabela 11, Elabela 22, or Elabela 32 for 1 h. Slides were mounted in fluorescence mounting medium (Dako, Carpinteria, CA, USA) and images were taken by using a Zeiss LSM-780 confocal microscope (Zeiss, Jena, Germany) that was equipped with appropriate laser lines and filters sets for 488 and 564 nm for fluorescence imaging. Images were acquired using a ×63 objective and digital zoom set to ×1.4. A minimum of 6 images were collected for each sample and analyzed with Zen browser software (Zeiss).

For fluorescence-based, high-throughput assay, U2OS cells that stably coexpressed hAPJ and β-arrestin 2-GFP were seeded on 384-well plates (3×10^3 cells/well). Twelve hours later, cells were starved for 1 h in phenol red–free minimum essential medium, and the different compounds from the libraries were added at a final concentration of 10 μM for 10 min before addition of apelin 13 at 10 nM final concentration. After 45 min of stimulation at 37°C, cells were fixed with paraformaldehyde (2% final) and images were acquired by using a Zeiss Axiovert 200 M fluorescent microscope. β-Arrestin 2-GFP aggregates were identified by Wavelet software, which evaluated the number and intensity of fluorescent dots as previously described (45).

Radioligand binding assay

Binding experiments were performed on permanently expressing hAPJ U2OS cells with [^{125}I]-apelin-13 as previously described (46). Results were analyzed with GraphPad Prism 5.0 using nonlinear regression to determine the K_i value of protamine. [^{3}H]-Dofetilide binding assays on human ether-a-go-go–related gene–expressing cells were carried out as reported previously by using 5 nM [^{3}H]-dofetilide (47).

Screening of protamine on different GPCRs

Activity of protamine was assessed on G_q-coupled receptors (angiotensin II receptor type 1, arginine vasopressin receptor 1A, oxytocin receptor, cholinergic receptor muscarinic 1, glutamate metabotropic receptor 1, and endothelin receptor type A) by using Ca^{2+} mobilization assay (Fluo-4 Direct Calcium Assay kit; Thermo Fisher Scientific) and on $G_{i/o}$-coupled receptors [C-X-C chemokine receptor type 4 (CXCR4) and cannabinoid receptor 1] by using split luciferase assay (GloSensor cAMP assay; Promega) according to manufacturer instructions.

Adenylyl cyclase assay

U2OS cells were seeded onto 24-well plates (25×10^3 cells/well). Forty-eight hours later, cells were washed twice with PBS, then incubated for 15 min at 37°C in 300 μl PBS medium that contained 1 mM magnesium acetate and 20 μM forskolin (Sigma-Aldrich) in the absence or presence of different doses of apelin 13 or protamine with apelin 13. After removal of the medium, the reaction was stopped by addition of 500 μl of a mixture of 95% methanol and 5% formic acid. The amount of cAMP was determined on cell lysates by a radioimmunoassay performed in mAb-coated tubes and using a [^{125}I]-labeled cAMP tracer (Immunotech, Thornwood, NY, USA) as described (37).

Western blot analysis

Subconfluent U2OS cells were serum-deprived for 18 h. In time course experiments, cells were stimulated at 37°C with 100 nM apelin 13 at different time points. For determining protamine

antagonist activity, cells were pretreated for 5 min with 1 μM protamine, then stimulated with 100 nM apelin for 5 min or treated with protamine alone for 10 min at 37°C. After treatments, cells were washed once in ice-cold PBS and lysed for 15 min on ice as previously described (10). Proteins (20 μg) were fractionated on 12% SDS-polyacrylamide gels and blotted to Protran nitrocellulose membranes (Schleicher and Schuell, Dassel, Germany). Membranes were stained with ponceau red and sliced horizontally so that several proteins could be probed on 1 blot. After blocking in Tris-buffered saline and Tween 20 buffer (50 mM Tris-HCl, pH 7.4, 150 mM NaCl, and 0.2% Tween 20) with 5% nonfat milk for 1 h at room temperature, membranes were incubated overnight at 4°C with blocking solution that contained the indicated Ab. Membranes were then washed and incubated with a horseradish peroxidase–conjugated secondary Ab and horseradish peroxidase activity was detected by using an ECL RevelBlot Plus kit (Ozyme).

Chick chorioallantoic membrane assay

Fertilized chicken eggs (E.A.R.L. Morizeau, Dangers, France) were incubated at 37°C in a humidified chamber. At d 3 of development, a window was made in the eggshell and sealed with Durapore tape (3M, St. Paul, MN, USA). At d 10, plastic coverslips (Thermanox; Thermo Fisher Scientific) that contained dried VEGF (500 ng) or apelin 13 (50 ng) with or without 15 μg protamine were deposited on the surface of the chicken embryo chorioallantoic membrane (CAM). After 4 d of incubation, coverslips and the attached CAM were excised and washed with PBS. Blood vessels were visualized by using fluorescein-labeled *Sambucus nigra* lectin (Vector Laboratories, Burlingame, CA, USA). Images were taken by using an Eclipse E400 microscope (Nikon, Toyko, Japan), and avascular *vs.* vascularized zones were quantified by using Explora Nova Morpho Expert/Mosaic Software (Explora Nova, La Rochelle, France)

Tumor model

When protamine was administered subcutaneously, a total of 1.5×10^5 TS/A cells that overexpressed apelin [as described in Sorli *et al.* (34)] were injected subcutaneously into the flank of BALB/c syngeneic mice. From the third day after TS/A cell injection, mice were treated with saline solution or protamine (5000 U/kg) twice per day.

When protamine treatment was injected intravenously, the experimental protocol was different. Mice were anesthetized with isoflurane/oxygen inhalation (2/98%). A catheter was introduced into the femoral vein, sealed under the back skin, and externalized in the interscapular region. The surgical procedure was carried out under aseptic conditions. Mice were individually housed and allowed to recover for 1 wk. A total of 1.5×10^5 TS/A cells that overexpressed apelin [as described (34)] were then injected subcutaneously into the flank of 9-wk-old female BALB/c syngeneic mice. From the third day after TS/A cells injection, mice were treated intravenously with saline solution or protamine (5000 U/kg) twice per day.

For both mouse tumor models, mouse body weight and tumor volume were measured 3 times/wk using the following formula: length × width^2 ×π/6.

Oral glucose tolerance test

Mice were anesthetized with isoflurane/oxygen inhalation (2/98%). A catheter was inserted into the femoral vein, sealed under the back skin, and externalized in the interscapular region. The surgical procedure was carried out under aseptic conditions. Mice were individually housed and allowed to recover for 1 wk. All drugs were injected as a bolus of 10 μl followed by a bolus of 10 μl of saline solution. On the day of the experiment, food was withheld from mice for 6 h. Conscious mice were intravenously injected with protamine (10 U/kg) or saline solution. Three minutes later and 30 min before oral glucose load (3 g/kg), apelin 13 (200 pmol/kg) or saline solution was injected. Blood was collected from the tail vein at −30, 0, 15, 30, 45, 60, 90, and 120 min after oral glucose load and glycemia was measured with a glucometer (Accu-Chek Performa; Roche, Basel, Switzerland). Blood was also collected 30 min before glucose load and 15 min after for plasma insulin concentrations.

In vivo blood pressure measurement using telemetry

Mice were anesthetized with isoflurane/oxygen inhalation (2/98%), and blood pressure measurements were performed by TA11PA-C10 transmitters (Data Sciences International, St. Paul, MN, USA).

After shaving and disinfecting the mouse neck, the left common carotid artery was isolated. The transmitter's catheter was inserted into the carotid artery and pushed forward until the tip entered the aortic arch. The transmitter's body was placed under the skin on the right flank of the mouse. For drug injections, a catheter was inserted into the femoral vein, sealed under the back skin, and externalized in the interscapular region. Mice were individually housed and allowed to recover for 1 wk. On the day of the experiment, food was withheld from mice for 6 h, and animals were anesthetized with isoflurane/oxygen inhalation (2/98%), and blood pressure was allowed to stabilize. Basal blood pressure was stabilized at 85.3 ± 1.9 mmHg, and heart rate was 475 ± 26 beats per minute. Mice were then injected with drugs as a bolus of 10 μl followed by a bolus of 10 μl of saline solution. Mice were pretreated with saline solution or protamine (700 U/kg) or a combination of protamine (700 U/kg) and heparin (1400 U/kg). Three minutes later, a saline solution or apelin 12 (100 nmol/kg) was injected. Data were recorded and analyzed by using Ponemah software (Data Sciences International). As previously described (48), each animal received an intravenous injection of angiotensin II (35 ng/kg) to determine responsiveness. Only those that experienced a response of an increase above 20 mmHg mean arterial pressure were used for bioassays of apelin, protamine, and heparin.

Statistical analysis

Results are expressed as means ± SEM. The sample size reported in each figure legend refers to the number of independently performed biologic replicates in the data set. All data points that could be analyzed were included in statistical analyses. No statistical methods were used to predetermine sample size. For experimental methods that were highly reproducible, such as oral glucose tolerance test, 7–8 biologic replicates were sufficient to detect effects of the compounds with $P < 0.05$. Experimental methods with greater variability between replicates, such as CAM assays or tumor growth, 15–25 biologic replicates were required to attain statistical significance between groups with $P < 0.01$. The investigators were not blinded to allocation during experiments and outcome assessment. Graphs and statistical analyses were performed by using GraphPad Prism 5. Gaussian distribution of data and equality of variances were tested with *F* Test and D'Agostino-Pearson normality test. Statistical tests performed are indicated in figure legends. Sigmoid curves from concentration-response experiments were analyzed by using nonlinear curve fitting. Experiments were not randomized.

RESULTS

Identification of protamine as an antagonist of APJ

To identify APJ antagonists, we engineered the human osteosarcoma U2OS cell line to permanently coexpress hAPJ and β-arrestin 2 tagged with GFP. These cells are large and flat and grow as a uniform monolayer, which makes them a useful model for fluorescence microscopy screening. In these cells, stimulation with a fluorescent apelin (apelin-TAMRA) induced formation of intracellular puncta composed of apelin-TAMRA/hAPJ/β-arrestin 2-GFP (**Fig. 1*A***). This approach is sensitive enough to quantify intracellular puncta induced by increasing apelin concentrations (Fig. 1*B*, *C*). Thus, apelin induced formation of cytosolic clusters of APJ complexes in APJ/β-arrestin 2-GFP upon exposure to ligand with an EC_{50} of $1.65 \pm 1.2 \times 10^{-9}$ M (Fig. 1*C*). Consequently, we set up a high-throughput screening assay and tested both the John Hopkins Drug Library that contained FDA-approved molecules (1514 compounds) and the combinatorial library from Tripos (50,000 compounds). Among the different compounds tested, we identified protamine as an antagonist of APJ internalization induced by apelin (Fig. 1*B* and Supplemental Table 1). In our screen, protamine inhibited in a dose-dependent manner the internalization of APJ in complex with β-arrestin 2-GFP induced by 10 nM of apelin with an IC_{50} of $315.3 \pm 1.7 \times 10^{-9}$ M (Fig. 1*D*). As this fluorescence-microscopy approach may produce false positives, we decided to confirm that APJ could bind to protamine. The affinity of protamine for APJ was studied by assessing its ability to displace [^{125}I]-apelin-13 binding on U2OS cells that stably expressed hAPJ receptor and β-arrestin 2-GFP. We first determined the apparent dissociation constant K_d of [^{125}I]-apelin-13 on these cells by performing saturation curves. Whereas [^{125}I]-apelin-13 was unable to specifically bind to vasopressin receptor, its K_d value for hAPJ receptor was 0.87×10^{-9} M (data not shown). In this assay, protamine dose-dependently inhibited specific binding of [^{125}I]-apelin-13 (0.5 nM) with a K_i value of 390×10^{-9} M (Fig. 1*E*).

A new endogenous ligand of APJ, Elabela/Toddler, has been recently identified. We thus measured the effect of protamine on Elabela-induced APJ activation in U2OS cells that stably expressed hAPJ receptor and β-arrestin 2-GFP. Whereas the different fragments of Elabela (Elabela 11, Elabela 22, and Elabela 32) induce β-arrestin 2-GFP recruitment to APJ and its internalization, pretreatment with protamine fully inhibited the effects of the different forms of Elabela (Supplemental Fig. 1). Thus, protamine fully antagonized APJ activation induced by the 2 natural ligands of APJ, apelin and Elabela.

To analyze the possible action of protamine on other cell-surface receptors, the activity of protamine on different GPCRs and ion channels was assessed. Among the different GPCRs tested (AT1aR, vasopressin V1a, oxytocin OTR, muscarinic m1R, chemokines CXCR4, metabotropic glutamate receptor 1, cannabinoid receptor type 1, and endothelin receptor type 1), no intrinsic activity of protamine was detected on these receptors. Moreover, assessment of the antagonist potency of protamine on these receptors showed no effect of protamine, except for CXCR4 receptor for which protamine inhibited SDF-1α activity by 88 ± 12.4% (Fig. 1*F*). Conversely, protamine did not displace binding of tritiated Dofetilide to human ether-a-go-go–related gene potassium channel (Supplemental Fig. 2).

Protamine antagonizes G-protein– and β-arrestin–dependent signaling pathways activated by apelin

We next analyzed the activity of protamine on the different signaling pathways that are activated by apelin. G_i-protein–mediated cAMP inhibition is the best-characterized response resulting from APJ activation. Thus, we first determined the intrinsic activity of protamine on cAMP production in U2OS cells that permanently expressed hAPJ and β-arrestin 2-GFP. In this assay, protamine acted as an inverse agonist on APJ, increasing cAMP accumulation induced by forskolin with an EC_{50} of $820 \pm 2 \times 10^{-9}$ M (**Fig. 2*A***). We then addressed the antagonist property of protamine on apelin-induced G_i signaling. As shown in Fig. 2*B*, protamine was able to dose-dependently block apelin effects with an IC_{50} of $462 \pm 1.7 \times 10^{-9}$ M. Downstream G_i protein pathway, it is well established that apelin activates ERK1/2 and Akt in different cell types (1, 7, 9, 10). The same results were obtained in U2OS cells that coexpressed hAPJ and β-arrestin 2-GFP, where apelin promoted a time-dependent phosphorylation of p42/p44 ERKs and Akt proteins (Fig. 2*C*). Whereas protamine did not induce ERK or Akt phosphorylation in these cells, it inhibited MAPK and Akt activation induced by apelin (Fig. 2*D*).

Given the potential importance of β-arrestin–mediated desensitization and internalization of APJ (7), we next evaluated the effect of protamine on β-arrestin recruitment to APJ. Thus, a BRET approach was developed by using HEK293T cells that transiently coexpressed hAPJ and β-arrestin 2 fused to their C terminus with Rluc, the BRET donor, or YFP (the yellow variant of EGFP), the BRET acceptor, respectively. By using real-time BRET measurement in cells that expressed only hAPJ-Rluc, we observed that apelin did not induce BRET variations compared with PBS-treated cells; however, in cells that coexpressed hAPJ-Rluc and β-arrestin 2-YFP, apelin rapidly increased BRET levels, which were stable for >30 min (Fig. 2*E*). Apelin-induced β-arrestin 2 recruitment to hAPJ in living cells was dose dependent, with an EC_{50} of $10.7 \pm 1.2 \times 10^{-9}$ M (Fig. 2*F*). Whereas protamine did not possess any intrinsic activity on β-arrestin 2 translocation to hAPJ as measured by BRET, apelin activity was fully inhibited dose dependently by protamine with an IC_{50} of $480.2 \pm 1.2 \times 10^{-9}$ M (Fig. 2*G*, *H*). As apelin can also promote β-arrestin 1 recruitment to APJ (7), we used the same BRET approach to evaluate the activity of apelin on β-arrestin 1 recruitment in our system and to determine the antagonist activity of protamine. Apelin induced β-arrestin 1 recruitment to hAPJ with an EC_{50} of $33.7 \pm 1.4 \times 10^{-9}$ M in

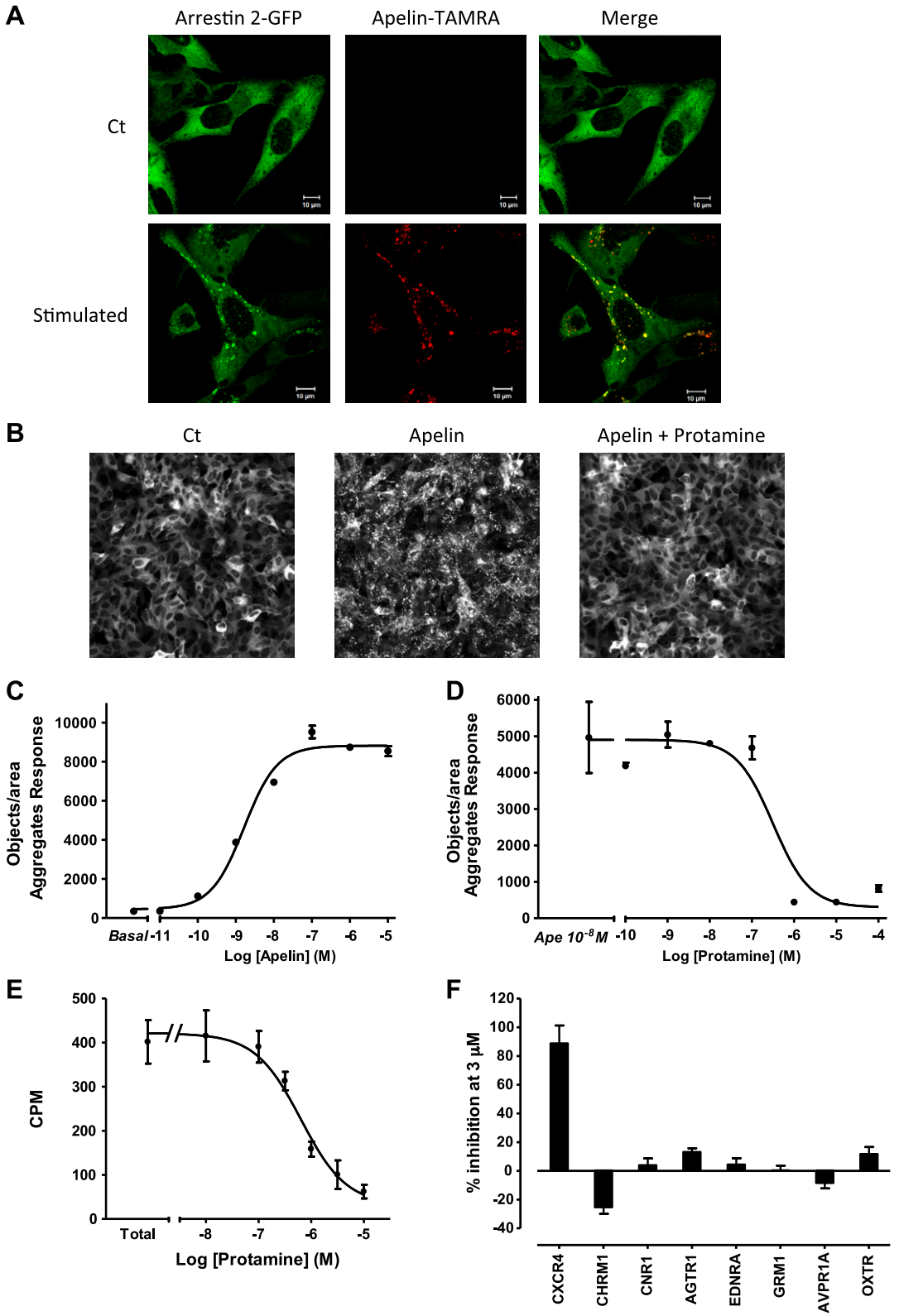

Figure 1. Identification of protamine as an antagonist of APJ. *A*) Confocal pictures of U2OS cells that stably expressed APJ and β-arrestin 2-GFP stimulated with PBS (upper) or with fluorescent apelin-TAMRA (10 nM) for 1 h. Apelin-TAMRA treatment induces internalization of APJ/β-arrestin 2-GFP in complex with apelin-TAMRA. Green channel illustrates the localization of β-arrestin 2-GFP, whereas the red channel shows apelin-TAMRA, highlighting only internalized apelin-TAMRA. Scale bar, 10 µm. *B*) Images from microscopy-based screening in 384-well plates. U2OS cells that stably expressed APJ and β-arrestin 2-GFP were treated with PBS (left), apelin 13 (10 nM; middle), or with protamine (1 µM) and apelin 13 (10 nM; right) for 45 min. *C*) Quantification of aggregates created by the formation of intracellular clusters of APJ/β-arrestin 2-GFP after a dose response of apelin 13 in U2OS cells that stably expressed APJ and β-arrestin 2-GFP. *D*) Protamine dose-dependently inhibits formation

(*continued on next page*)

HEK293T cells that coexpressed hAPJ-Rluc and β-arrestin 1-YFP (Supplemental Fig. 3*A*). In addition, whereas protamine had no intrinsic agonistic activity, it inhibited, in a dose-dependent manner, apelin-induced β-arrestin 1 translocation to hAPJ, with an IC_{50} 480 ± 1.9 × 10^{-9} M (Supplemental Fig. 3*B*, *C*).

Protamine is an arginine-rich basic protein that can form a stable complex with the negatively charged heparin. To further confirm that protamine antagonism is not mediated *via* its positive charges, the effect of poly-D-lysine on hAPJ was measured. Poly-D-lysine had no intrinsic activity on β-arrestin 2 recruitment, and a high dose of this positively charged polymer did not inhibit apelin-induced β-arrestin 2 recruitment to hAPJ (Supplemental Fig. 4*A*, *B*).

Taken together, our data demonstrate that protamine acts as an antagonist of hAPJ by displacing apelin binding and abrogating G-protein activation and β-arrestin recruitment.

APJ, also called angiotensin receptor-like 1, shares strong sequence homology with AT1aR (54% in transmembrane domains and 31% for the entire sequence) (1). We previously showed that protamine does not inhibit G_q protein activation induced by angiotensin II (Fig. 1*F*); therefore, we analyzed the activity of protamine on β-arrestin recruitment to AT1aR and its ability to antagonize angiotensin II effects. The same BRET approach used for hAPJ was used in HEK293T cells that coexpressed AT1-Rluc and β-arrestin 2-YFP. In these cells, angiotensin II dose-dependently induced β-arrestin 2 recruitment to AT1aR with an EC_{50} of 24 ± 1.4 × 10^{-9} M, whereas protamine was inactive at modifying BRET levels (Supplemental Fig. 5*A*, *B*); however, protamine was unable to antagonize β-arrestin 2-YFP translocation to AT1aR induced by angiotensin II (Supplemental Fig. 5*C*).

Antagonist activity of protamine can be reversed by heparin

Protamine sulfate, which possesses a high affinity for heparin, is routinely used in clinic after heart surgery to reverse the anticlotting effects of heparin. Consequently, we assumed that heparin could inhibit the antagonist activity of protamine on APJ. To validate our hypothesis, we first studied the intrinsic agonistic activity of heparin and its effect on apelin-stimulating hAPJ. By using the previously described BRET assay, we showed that heparin did not induce β-arrestin 2 recruitment to hAPJ (**Fig. 3*A***). Furthermore, it did not inhibit β-arrestin 2 recruitment to hAPJ induced by apelin (Fig. 3*B*). Consequently, we next tested the effect of heparin on protamine antagonizing apelin activity. For this purpose, real-time BRET monitoring of β-arrestin 2-YFP recruitment to hAPJ-Rluc was realized in HEK293T cells. By using this approach, we demonstrated that protamine did not induce β-arrestin 2 translocation to hAPJ over time but instead fully inhibited apelin activity when apelin was added few minutes later. Surprisingly, injection of heparin after apelin immediately reversed antagonist activity of protamine. As a result, apelin that was present in the medium can bind hAPJ and induced β-arrestin 2-YFP translocation (Fig. 3*C*). Moreover, our data demonstrate that the reverse activity of heparin on protamine is dose-dependent (Fig. 3*D*). Accordingly, our results clearly show that protamine can antagonize APJ activation, and this effect can be reversed by heparin, which can release protamine that is bound to APJ.

Antiangiogenic and antitumor activities of protamine are mediated *via* antagonism of APJ

Since the early 1980s, protamine has been described as a potent inhibitor of angiogenesis *in vitro* and *in vivo* as well as in different mouse models of cancer (49, 50). Of interest, this antiangiogenic activity is fully prevented by heparin cotreatment (50). Regarding angiogenesis, the role of apelin signaling is well documented. This angiogenic peptide plays a crucial role in both physiologic and pathophysiologic angiogenesis, such as tumor neovascularization (25, 34, 36, 38, 40); therefore, we evaluated whether protamine could inhibit apelin-induced angiogenesis in the CAM assay system. In this experimental model, we show that apelin induced a strong increase in vessel density and a reduction of the intercapillary space similar to that obtained with VEGF. Conversely, protamine applied alone on the CAM did not modify vessel density compared with control. Of interest, protamine inhibited apelin-induced angiogenesis, whereas it did not alter the angiogenic effect of VEGF (**Fig. 4*A*, *B***).

To further examine the activity of protamine on tumor growth induced by apelin, a syngeneic mouse tumor model was developed by using TS/A mammary carcinoma cells that stably overexpressed apelin (TS/A-apelin). As previously described, these cells do not express APJ, and apelin overexpression accelerates *in vivo* tumor growth by inducing tumor neoangiogenesis (34). TS/A-apelin cells were implanted subdermally into the flanks of BALB/c mice and animals were then treated subcutaneously with protamine or saline twice per day. During the early stage of tumor development,

of APJ/ β-arrestin 2-GFP intracellular clusters induced by apelin 13 (10 nM) in U2OS cells that expressed APJ and β-arrestin 2-GFP. Data represent means ± SEM of 2 independent experiments (*C*, *D*) or are representative of 6 (*A*) and 2 (*B*) independent experiments. *E*) Protamine displaces binding of [^{125}I]-apelin 13 (0.5 nM) to APJ in a dose-dependent manner. Results were analyzed by nonlinear regression on a pooled data set from 2 independent experiments, assuming a model with 1-site competitive binding (GraphPad Prism 5.0). *F*) GPCR profiling panel for protamine. Antagonist activity of protamine was assessed on different G_q- and $G_{i/o}$-coupled receptors. Data represent means ± SEM of 3 independent experiments. AGTR1, angiotensin II receptor type 1; AVPR1A, arginine vasopressin receptor 1 A; CHRM1, cholinergic receptor muscarinic 1; CNR1, cannabinoid receptor 1; CXCR4, C-X-C chemokine receptor type 4; EDNRA, endothelin receptor type A; GRM1, glutamate metabotropic receptor 1; OXTR, oxytocin receptor.

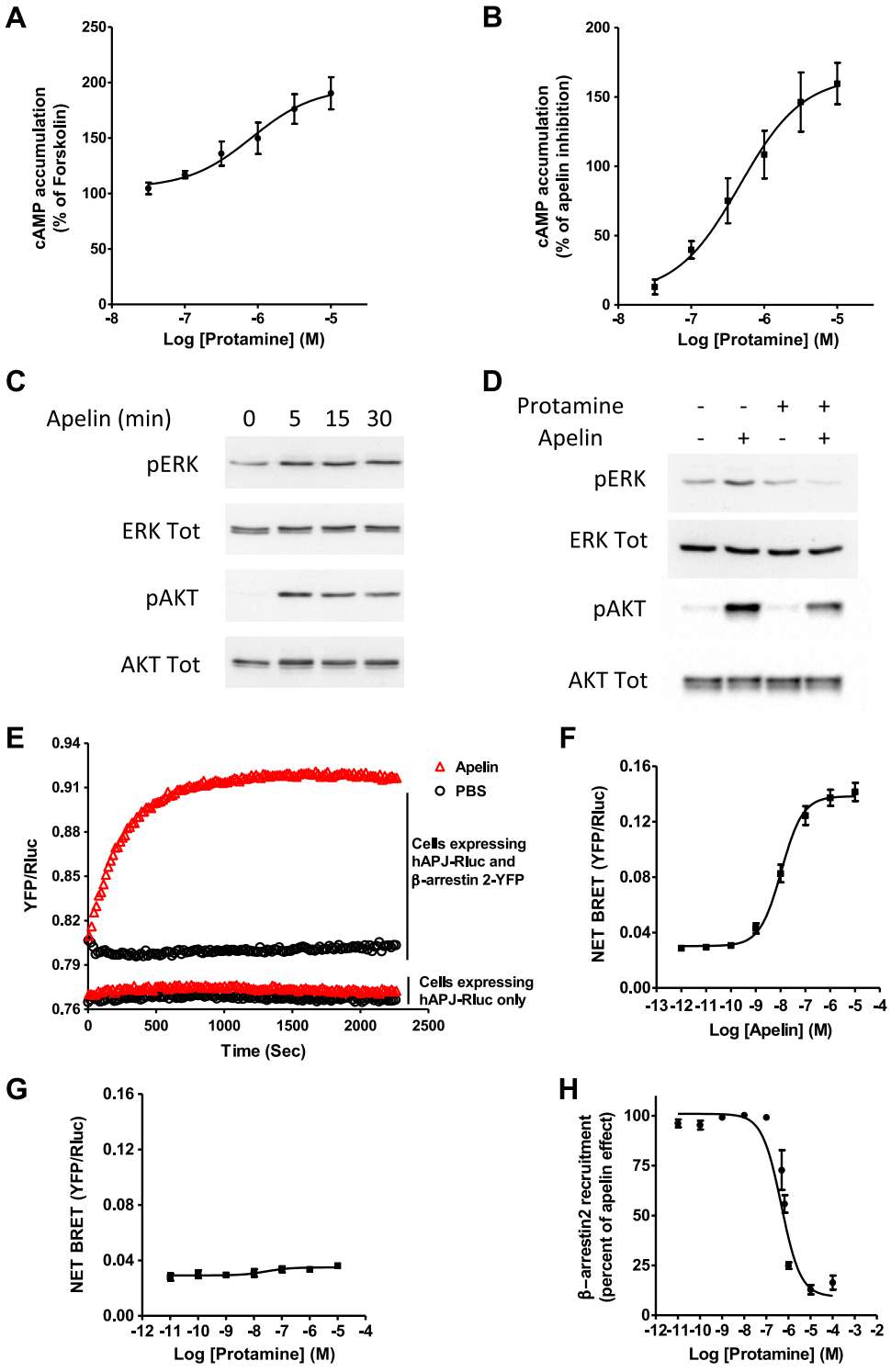

Figure 2. Antagonist activity of protamine on intracellular responses induced by apelin. *A*) Intrinsic activity of protamine on $G_{i/o}$ activation *via* APJ. U2OS cells that stably expressed hAPJ and β-arrestin 2-GFP were stimulated with protamine in the presence of forskolin (20 μM). cAMP production was normalized to the percentage of forskolin-stimulated cAMP accumulation (set at 100%). *B*) Dose-response curve of protamine for blocking adenylyl cyclase inhibition induced by apelin 13 (10 nM) in the presence of forskolin (20 μM). *C*) Apelin 13 (100 nM) promotes time-dependent phosphorylation of p42/p44 ERKs and Akt proteins in U2OS cells that stably expressed hAPJ and β-arrestin 2-GFP. *D*) Protamine pretreatment (1 μM) inhibits ERKs and Akt phosphorylation induced by apelin 13 (100 nM) in the U2OS cells that expressed hAPJ and β-arrestin 2-GFP. *E*) Real-time measurement of β-arrestin 2 recruitment to APJ measured by BRET in HEK293T cells that expressed hAPJ-Rluc and β-arrestin 2-YFP after addition, at time 0, of 1 μM apelin 13 (△) or PBS (O). As a negative control, similar experiments were carried out on cells that transiently expressed only Rluc-tagged hAPJ. *F*, *G*) Dose-response curve of apelin 13 (*F*) or protamine (*G*) for β-arrestin 2 recruitment to APJ measured by BRET in HEK293T cells that transiently coexpressed hAPJ-Rluc and β-arrestin 2-YFP. *H*) Protamine dose-dependently inhibits β-arrestin 2 recruitment to APJ induced by apelin 13 (100 nM). Data are expressed as the percentage of the maximal BRET signal obtained in HEK293T cells that transiently coexpressed Rluc-tagged hAPJ and YFP-tagged β-arrestin 2 stimulated with apelin 13 at 100 nM (100%). Data represent means ± SEM of 5 (*A*, *B*), 21 (*F*), 6 (*G*), and 4 (*H*) independent experiments or are representative of 1 experiment performed 3 times independently (*C*, *D*, *E*).

protamine significantly reduced the accumulated tumor burden per animal by 50% (Fig. 4C). However, the protamine-induced decrease of tumor development disappeared in the later stages, and a regrowth of the protamine-treated tumors was observed. Of importance, this activity of protamine on tumor growth did not depend on the drug administration route as the same effects were observed after intravenous injection of protamine (Supplemental Fig. 6).

Protamine inhibits *in vivo* glucose tolerance and vasodilatation induced by apelin, and its activity is reversed by heparin

To show that protamine also inhibits apelin effects *in vivo*, we next analyzed protamine activity on glucose utilization and vasodilatation induced by apelin. As previously described during an oral glucose tolerance test (8), amplitude of hyperglycemic response was significantly reduced

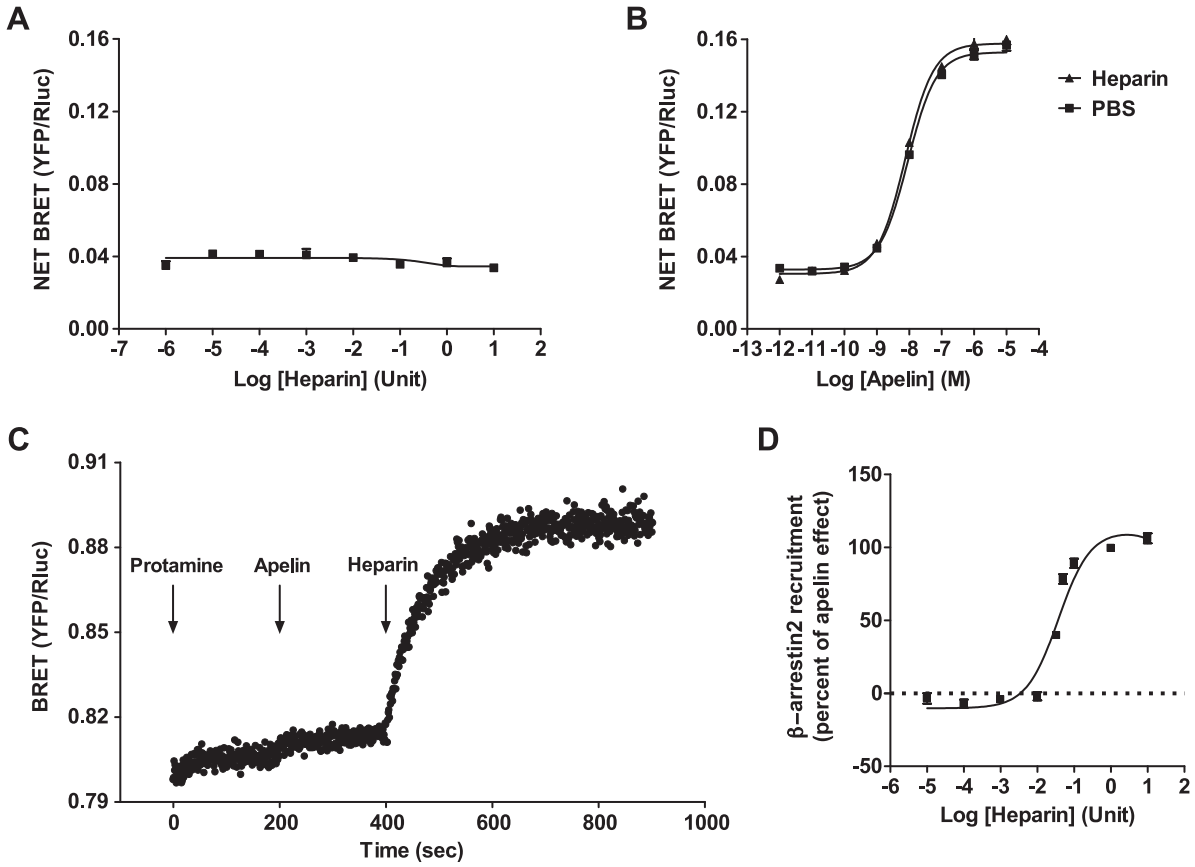

Figure 3. Heparin reverses antagonist activity of protamine on APJ. *A*) Dose-response curve (U/100 μl) of heparin for β-arrestin 2 recruitment to APJ was measured by BRET in HEK293T cells that transiently coexpressed APJ-Rluc and β-arrestin 2-YFP. *B*) Heparin (10 U/100 μl) does not modify apelin 13–induced β-arrestin 2 recruitment to APJ in HEK293T cells that expressed APJ-Rluc and β-arrestin 2-YFP and measured by BRET. *C*) Real-time measurement of BRET signal in HEK293T cells that coexpressed APJ-Rluc and β-arrestin 2-YFP after addition of protamine (100 μM) at time 0, followed by injection of apelin 13 (1 μM) at time 200 s. Heparin (10 U/100 μl) was added 200 s later. *D*) Heparin dose-dependently reverses antagonist activity of protamine (1 μM) on β-arrestin 2 recruitment to APJ induced by apelin 13 (100 nM). Data are presented as the percentage of the maximal inhibition obtained with protamine. Data represent means ± SEM of 3 (*A*), 6 (*B*), and 4 (*D*) independent experiments each performed in duplicate or are representative of 1 experiment performed 3 times independently (*C*).

when animals received an intravenous injection of 200 pmol/kg of apelin compared with saline-treated mice (**Fig. 5**). Whereas protamine alone had no significant effect on glycemia, it clearly abrogated apelin effects. Of interest, neither apelin, protamine, nor a combination of protamine and apelin altered plasma insulin levels, which suggested that none of these treatments has any effect on insulin secretion (Supplemental Fig. 7).

In addition to its beneficial effect on glucose homeostasis, systemic administration of apelin lowers arterial blood pressure *via* activation of APJ expressed by endothelial cells (24). We thus assessed protamine effects on apelin-induced vasodilatation in mice. Anesthetized animals were injected i.v with the different compounds *via* the femoral vein, and arterial blood pressure was monitored over time. Whereas vehicle injection of 0.9% saline revealed no change in blood pressure (Supplemental Fig. 8), angiotensin II elicited an immediate increase in mean arterial pressure, with a maximum of 37.3 ± 5.3 mmHg, 1 min after its injection (**Fig. 6**). Conversely, administration of apelin induced a transient and significant decrease in mean arterial pressure, reaching −22 ± 3.8 mmHg at approximately 1.0–1.5 min after treatment, without changing heart rate (data not shown). This apelin effect was blunted when animals were pretreated with protamine (Fig. 6), whereas protamine did not modify blood pressure by itself (Supplemental Fig. 8). As our previous results demonstrate that heparin can reverse antagonist activity of protamine on APJ *in vitro* (Fig. 3*C*, *D*), we next evaluated the effect of heparin on the antagonism mediated by protamine on the hypotensive effect of apelin. For this purpose, heparin was coinjected with protamine a few minutes before apelin treatment. Whereas heparin alone or heparin plus protamine did not modify mean arterial pressure (Supplemental Fig. 8), heparin fully counteracted protamine antagonist activity, thereby restoring the hypotensive effect of apelin (Fig. 6).

DISCUSSION

By using an original fluorescence-based, high-throughput screening on the basis of the ability of APJ to internalize

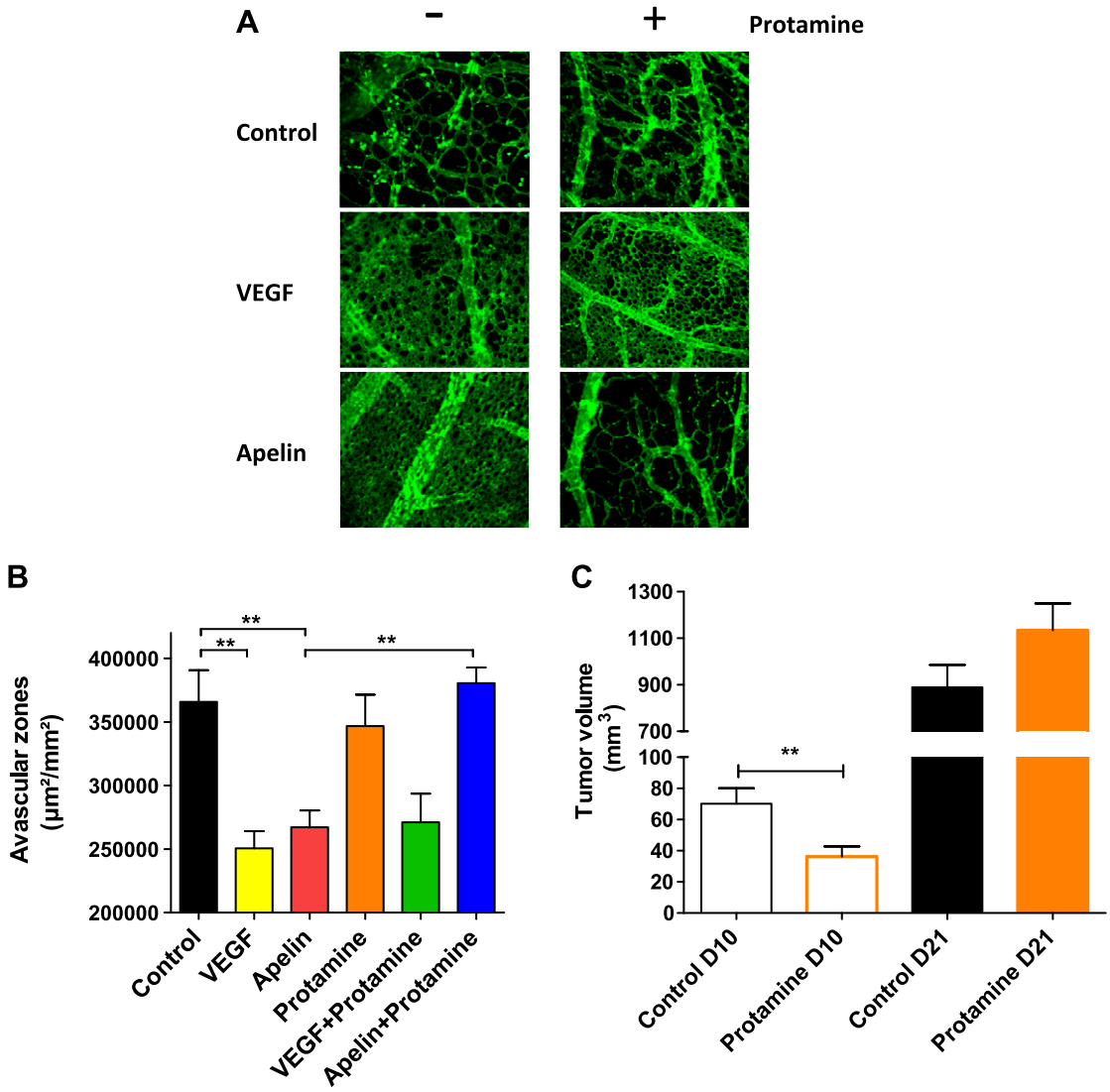

Figure 4. Antiangiogenic and antitumor activity of protamine is mediated *via* antagonism of APJ. *A*) Images of representative CAMs for each condition [PBS, top; $VEGF_{165}$ (500 ng), middle; apelin 13 (50 ng), bottom] are shown in the absence (left) or presence of protamine (15 µg; right). Blood vessels (green) are visualized by using fluorescein-labeled *S. nigra* lectin. *B*) Angiogenic activity of apelin and VEGF and antiangiogenic activity of protamine were quantified by measuring the surface of avascular zones in the CAM assay. Data represent means ± SEM of 20 (control, apelin, and VEGF + protamine), 15 (VEGF and protamine alone), and 25 (apelin + protamine) CAMs. Statistical significance was assessed by using 1-way ANOVA followed by Bonferroni posttest. $^{**}P < 0.01$. *C*) Effect of subcutaneous injection of protamine (5000 U/kg) twice per day on tumor volume (TS/A tumor cell line overexpressing apelin) compared with saline solution–treated mice. Tumor volume on days (D) 10 and 21 are presented. Statistical significance was assessed by using unpaired Student's *t* test. $^{**}P < 0.01$; $n = 17$ animals per group.

with GFP-tagged β-arrestin 2, we report here the isolation of a new antagonist of APJ, protamine, which displays an affinity of 390 nM for hAPJ. Whereas protamine has no intrinsic activity on β-arrestin recruitment to hAPJ and does not activate Akt or ERKs, it acts as an inverse agonist on the $G_{i/o}$ pathway. Conversely, protamine behaves as a full antagonist, inhibiting these different signaling pathways with comparable IC_{50} values. Such antagonist effects of protamine were also confirmed *in vivo* on apelin-induced vasodilatation and glucose tolerance. Of interest, APJ blockade was fully and swiftly reversed after heparin administration both *in vitro* and *in vivo*.

To date, few APJ antagonists have been identified. The peptide analog, apelin F13A, was first described to inhibit apelin 13–induced decrease in blood pressure and splanchnic neovascularization (48, 51); however, apelin F13A can also behave as an APJ agonist on different *in vitro* functional assays (1). Another peptide, MM54, is a competitive antagonist of hAPJ, with a K_i of 82 nM, and does not bind to AT1aR (42); however, unlike protamine, which has been clinically approved by the FDA, the efficacy of MM54 remains to be established in human patients.

At the chemical level, protamine is an arginine-rich basic protein, similar to the compound ALX 40-4C, a polypeptide of 9 arginine residues, which behaves as an hAPJ antagonist in the micromolar range (43). Of interest, poly-D-lysine, which possesses a similar structure and charge density compared with protamine, does not inhibit

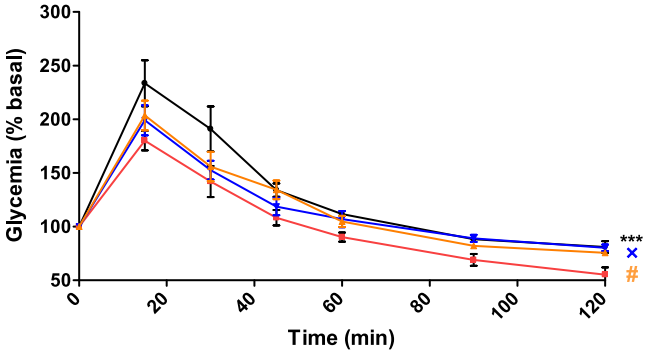

Figure 5. Protamine inhibits apelin-induced glucose tolerance. Oral glucose tolerance test in mice denied food for 6 h that were intravenously treated with saline (black curve, n = 8), apelin 13 (200 pmol/kg; red curve, n = 5), protamine (10 U/kg), and apelin 13 (200 pmol/kg; blue curve, n = 7), or with protamine alone (10 U/kg; orange curve, n = 5) 30 min before oral glucose (3 g/kg) load (time 0). Blood was collected from the tail vein at −30, 0, 15, 45, 30, 60, 90, and 120 min, and glycemia was measured on these samples. Each point shows the mean ± SEM of the described number of mice. Data were analyzed by using 1-way ANOVA repeated measurements. $^{***}P < 0.001$, apelin *vs.* saline solution; $^{\#}P < 0.05$, apelin *vs.* protamine; $^{\times}P < 0.05$, apelin *vs.* protamine + apelin.

hAPJ stimulation by apelin, which suggests that binding to hAPJ and activity of protamine do not rely on its positive charges. However, like ALX 40-4C, which antagonizes C-X-C chemokine receptor type 4 in the nanomolar range, protamine also inhibits SDF-1α activity on this receptor *in vitro*; therefore, the antiangiogenic and antitumor activities of protamine could rely on antagonism at both APJ and CXCR4. However, more experiments are needed to confirm the involvement of CXCR4 in protamine effects *in vivo*.

Given the structural relationship between APJ and AT1aR (2, 3), it should be noted that protamine alone does not activate angiotensin receptor, nor does it inhibit its stimulation by angiotensin II. Surprisingly, protamine has been observed to bind fibroblast growth factor and platelet-derived growth factor tyrosine kinase receptors and inhibit their mitogenic activity in endothelial and fibroblast cells, respectively (52, 53); however, even a 100-fold molar excess of protamine does not impair basic fibroblast growth factor mitogenic activity in endothelial cells (53). Regarding platelet-derived growth factor receptors, the precise K_i value and efficacy of protamine have not been evaluated by Huang and collaborators (52).

At the clinical level, the first clinical indication of protamine is to reverse the anticlotting action of heparin. This effect relies on direct interaction between the 2 proteins *via* opposite charges. Conversely, our results demonstrate that heparin can also reverse the effects of protamine, even when it is bound to the receptor, which suggests that the interaction between heparin and protamine involves regions of protamine that are still accessible.

Several decades ago, protamine was described as an antiangiogenic molecule that was able to reduce vascular density and tumor growth in different mouse models of cancer (49, 50). In addition, such an antitumor effect has also been reported in patients with advanced carcinoma (54). These properties are confirmed in our syngeneic apelin-overexpressing mouse tumor model, TS/A-apelin, where protamine reduced the accumulated tumor burden in the early stages of tumor development. Of interest, prolonged treatment of animals revealed a regrowth of protamine-treated tumors. Such a resistance is similar to that observed with antiangiogenic treatments, such as antibodies that target either VEGF receptor (55) or VEGF with bevacizumab (avastin) as monotherapy in a clinical trial (56). This effect is explained by activation of other angiogenic pathways to circumvent the blockade of the targeted pathway (55). One possible angiogenic candidate would be the VEGF pathway, given that protamine is ineffective at inhibiting its proangiogenic activity in the CAM assay. In addition to its action on tumor neoangiogenesis, protamine could also target apelin signaling function at the tumor cell level. Indeed, as apelin and APJ are expressed by human carcinoma cells, apelin can promote their survival and proliferation (35–37); however, in our mouse TS/A tumor model, the activity of protamine was only analyzed on tumor angiogenesis and not in

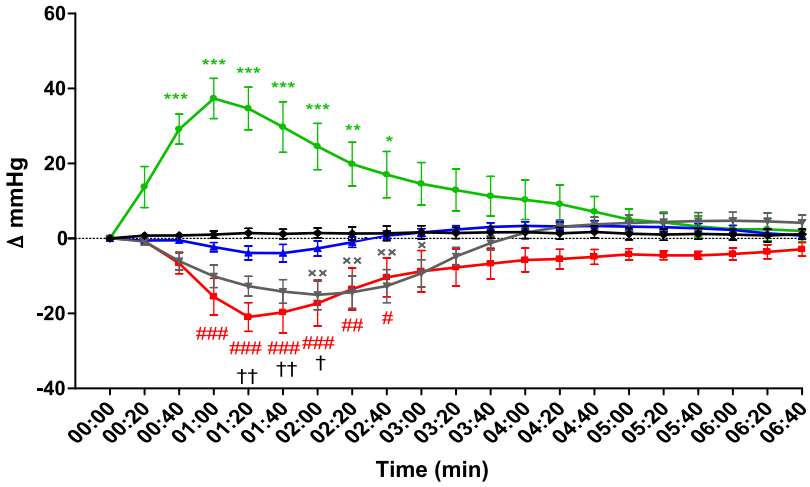

Figure 6. Protamine inhibits apelin-induced vasodilatation, and its activity can be reversed by heparin. Time-dependent changes of arterial blood pressure after intravenous administration at time 0 of saline (black curve, n = 5); angiotensin II (35 ng/kg; green curve, n = 5); apelin 12 (100 nmol/kg; red curve, n = 5); protamine (700 U/kg) and apelin 12 (100 nmol/kg; blue curve, n = 5); and heparin (1400 U/kg), protamine (700 U/kg), and apelin 12 (100 nmol/kg; gray curve, n = 5). Data represent means ± SEM. Statistical significance between groups was assessed by using 2-way ANOVA followed by Bonferroni posttest. $^{*}P < 0.05$, $^{**}P < 0.01$, $^{***}P < 0.001$, angiotensin *vs.* saline solution; $^{\#}P < 0.05$, $^{\#\#}P < 0.01$, $^{\#\#\#}P < 0.001$, apelin *vs.* saline solution; $^{\dagger}P < 0.05$, $^{\dagger\dagger}P < 0.01$, protamine + apelin *vs.* apelin; $^{\times}P < 0.05$, $^{\times\times}P < 0.01$, heparin + protamine + apelin *vs.* protamine + apelin.

tumor cells as this cell line was reported to not express APJ (34). Accordingly, it is likely that protamine effects on tumor growth are underestimated in the results presented here.

In addition to counteracting the anticlotting effects of heparin after cardiac surgery, protamine has side effects that lead to increased pulmonary artery pressure secondary to pulmonary vasoconstriction. Of interest, patients with pulmonary hypertension display a significant reduction of serum apelin levels compared with healthy controls (28), together with a down-regulation of apelin expression in pulmonary arterial endothelial cells (57). Moreover, apelin-null mice develop more severe pulmonary hypertension compared with wild-type mice when exposed to chronic hypoxia (28). Thus, it is likely that pulmonary hypertension induced by protamine in clinic may also rely on the inhibition of APJ. Further experiments will be necessary to assess the potency of apelin to reverse this adverse effect of protamine.

Altogether, our data reveal a new pharmacologic property of protamine, the blockade of APJ, which could explain some side effects that have been observed in protamine-treated patients, and a new clinical indication, an antiangiogenic activity for treating neoangiogenesis-dependent diseases and cancer. FJ

ACKNOWLEDGMENTS

The authors thank Aurore Desquesnes from the phenotyping platform (Anexplo–US006/CREFRE) for technical assistance, the Cellular Imaging Facility of Rangueil (Toulouse, France), and Dr. Sean M. Peterson (Duke University Medical Center) for helpful discussions. This work was supported by Ligue Régionale Midi Pyrénées Contre le Cancer (R12018BB/RAB12003BBA), Cancéropole GSO Emergence (R11109BB/RPS11008BBA), and an ATCS-AO1 Grant from Toulouse University (to B.M.). During the initial stages of this work, B.M. was recipient of a Marie Curie Outgoing International Fellowship of the European Commission (FP6-2005-Mobility-6). The authors declare no conflicts of interest.

AUTHOR CONTRIBUTIONS

S. Le Gonidec, Y. Audigier, and B. Masri designed research; S. Le Gonidec, C. Chaves-Almagro, H. J. Kang, X.-P. Huang, B. L. Roth, H. Prats, B. Knibiehler, L. S. Barak, M. G. Caron, P. Valet, Y. Audigier, and B. Masri analyzed data; S. Le Gonidec, C. Chaves-Almagro, Y. Bai, H. J. Kang, X.-P. Huang, A. Smith, E. Wanecq, Y. Audigier, and B. Masri performed research; and Y. Audigier and B. Masri wrote the paper.

REFERENCES

1. Chaves-Almagro, C., Castan-Laurell, I., Dray, C., Knauf, C., Valet, P., and Masri, B. (2015) Apelin receptors: from signaling to antidiabetic strategy. *Eur. J. Pharmacol.* **763**, 149–159
2. O'Dowd, B. F., Heiber, M., Chan, A., Heng, H. H., Tsui, L. C., Kennedy, J. L., Shi, X., Petronis, A., George, S. R., and Nguyen, T. (1993) A human gene that shows identity with the gene encoding the angiotensin receptor is located on chromosome 11. *Gene* **136**, 355–360
3. Masri, B., Knibiehler, B., and Audigier, Y. (2005) Apelin signalling: a promising pathway from cloning to pharmacology. *Cell. Signal.* **17**, 415–426
4. Tatemoto, K., Hosoya, M., Habata, Y., Fujii, R., Kakegawa, T., Zou, M. X., Kawamata, Y., Fukusumi, S., Hinuma, S., Kitada, C., Kurokawa, T., Onda, H., and Fujino, M. (1998) Isolation and characterization of a novel endogenous peptide ligand for the human APJ receptor. *Biochem. Biophys. Res. Commun.* **251**, 471–476
5. Habata, Y., Fujii, R., Hosoya, M., Fukusumi, S., Kawamata, Y., Hinuma, S., Kitada, C., Nishizawa, N., Murosaki, S., Kurokawa, T., Onda, H., Tatemoto, K., and Fujino, M. (1999) Apelin, the natural ligand of the orphan receptor APJ, is abundantly secreted in the colostrum. *Biochim. Biophys. Acta* **1452**, 25–35
6. Masri, B., Morin, N., Pedebernade, L., Knibiehler, B., and Audigier, Y. (2006) The apelin receptor is coupled to G_i1 or G_i2 protein and is differentially desensitized by apelin fragments. *J. Biol. Chem.* **281**, 18317–18326
7. Ceraudo, E., Galanth, C., Carpentier, E., Banegas-Font, I., Schonegge, A. M., Alvear-Perez, R., Iturrioz, X., Bouvier, M., and Llorens-Cortes, C. (2014) Biased signaling favoring gi over β-arrestin promoted by an apelin fragment lacking the C-terminal phenylalanine. *J. Biol. Chem.* **289**, 24599–24610
8. Dray, C., Knauf, C., Daviaud, D., Waget, A., Boucher, J., Buléon, M., Cani, P. D., Attané, C., Guigné, C., Carpéné, C., Burcelin, R., Castan-Laurell, I., and Valet, P. (2008) Apelin stimulates glucose utilization in normal and obese insulin-resistant mice. *Cell Metab.* **8**, 437–445
9. Masri, B., Lahlou, H., Mazarguil, H., Knibiehler, B., and Audigier, Y. (2002) Apelin (65-77) activates extracellular signal-regulated kinases *via* a PTX-sensitive G protein. *Biochem. Biophys. Res. Commun.* **290**, 539–545
10. Masri, B., Morin, N., Cornu, M., Knibiehler, B., and Audigier, Y. (2004) Apelin (65-77) activates p70 S6 kinase and is mitogenic for umbilical endothelial cells. *FASEB J.* **18**, 1909–1911
11. Chng, S. C., Ho, L., Tian, J., and Reversade, B. (2013) ELABELA: a hormone essential for heart development signals *via* the apelin receptor. *Dev. Cell* **27**, 672–680
12. Pauli, A., Norris, M. L., Valen, E., Chew, G. L., Gagnon, J. A., Zimmerman, S., Mitchell, A., Ma, J., Dubrulle, J., Reyon, D., Tsai, S. Q., Joung, J. K., Saghatelian, A., and Schier, A. F. (2014) Toddler: an embryonic signal that promotes cell movement *via* apelin receptors. *Science* **343**, 1248636
13. Ho, L., Tan, S. Y., Wee, S., Wu, Y., Tan, S. J., Ramakrishna, N. B., Chng, S. C., Nama, S., Szczerbinska, I., Chan, Y. S., Avery, S., Tsuneyoshi, N., Ng, H. H., Gunaratne, J., Dunn, N. R., and Reversade, B. (2015) ELABELA is an endogenous growth factor that sustains hESC self-renewal *via* the PI3K/AKT pathway. *Cell Stem Cell* **17**, 435–447
14. Wang, Z., Yu, D., Wang, M., Wang, Q., Kouznetsova, J., Yang, R., Qian, K., Wu, W., Shuldiner, A., Sztalryd, C., Zou, M., Zheng, W., and Gong, D. W. (2015) Elabela-apelin receptor signaling pathway is functional in mammalian systems. *Sci. Rep.* **5**, 8170
15. O'Carroll, A. M., Lolait, S. J., Harris, L. E., and Pope, G. R. (2013) The apelin receptor APJ: journey from an orphan to a multifaceted regulator of homeostasis. *J. Endocrinol.* **219**, R13–R35
16. De Mota, N., Reaux-Le Goazigo, A., El Messari, S., Chartrel, N., Roesch, D., Dujardin, C., Kordon, C., Vaudry, H., Moos, F., and Llorens-Cortes, C. (2004) Apelin, a potent diuretic neuropeptide counteracting vasopressin actions through inhibition of vasopressin neuron activity and vasopressin release. *Proc. Natl. Acad. Sci. USA* **101**, 10464–10469
17. Duparc, T., Colom, A., Cani, P. D., Massaly, N., Rastrelli, S., Drougard, A., Le Gonidec, S., Moulédous, L., Frances, B., Leclercq, I., Llorens-Cortes, C., Pospisilik, J. A., Delzenne, N. M., Valet, P., Castan-Laurell, I., and Knauf, C. (2011) Central apelin controls glucose homeostasis *via* a nitric oxide-dependent pathway in mice. *Antioxid. Redox Signal.* **15**, 1477–1496
18. Xin, Q., Cheng, B., Pan, Y., Liu, H., Yang, C., Chen, J., and Bai, B. (2015) Neuroprotective effects of apelin-13 on experimental ischemic stroke through suppression of inflammation. *Peptides* **63**, 55–62
19. Zeng, X. J., Yu, S. P., Zhang, L., and Wei, L. (2010) Neuroprotective effect of the endogenous neural peptide apelin in cultured mouse cortical neurons. *Exp. Cell Res.* **316**, 1773–1783
20. Bertrand, C., Valet, P., and Castan-Laurell, I. (2015) Apelin and energy metabolism. *Front. Physiol.* **6**, 115
21. Yue, P., Jin, H., Aillaud, M., Deng, A. C., Azuma, J., Asagami, T., Kundu, R. K., Reaven, G. M., Quertermous, T., and Tsao, P. S. (2010) Apelin is necessary for the maintenance of insulin sensitivity. *Am. J. Physiol. Endocrinol. Metab.* **298**, E59–E67

22. Szokodi, I., Tavi, P., Földes, G., Voutilainen-Myllylä, S., Ilves, M., Tokola, H., Pikkarainen, S., Piuhola, J., Rysä, J., Tóth, M., and Ruskoaho, H. (2002) Apelin, the novel endogenous ligand of the orphan receptor APJ, regulates cardiac contractility. *Circ. Res.* **91**, 434–440
23. Japp, A. G., Cruden, N. L., Amer, D. A., Li, V. K., Goudie, E. B., Johnston, N. R., Sharma, S., Neilson, I., Webb, D. J., Megson, I. L., Flapan, A. D., and Newby, D. E. (2008) Vascular effects of apelin *in vivo* in man. *J. Am. Coll. Cardiol.* **52**, 908–913
24. Ishida, J., Hashimoto, T., Hashimoto, Y., Nishiwaki, S., Iguchi, T., Harada, S., Sugaya, T., Matsuzaki, H., Yamamoto, R., Shiota, N., Okunishi, H., Kihara, M., Umemura, S., Sugiyama, F., Yagami, K., Kasuya, Y., Mochizuki, N., and Fukamizu, A. (2004) Regulatory roles for APJ, a seven-transmembrane receptor related to angiotensin-type 1 receptor in blood pressure *in vivo*. *J. Biol. Chem.* **279**, 26274–26279
25. Cox, C. M., D'Agostino, S. L., Miller, M. K., Heimark, R. L., and Krieg, P. A. (2006) Apelin, the ligand for the endothelial G-protein-coupled receptor, APJ, is a potent angiogenic factor required for normal vascular development of the frog embryo. *Dev. Biol.* **296**, 177–189
26. Chun, H. J., Ali, Z. A., Kojima, Y., Kundu, R. K., Sheikh, A. Y., Agrawal, R., Zheng, L., Leeper, N. J., Pearl, N. E., Patterson, A. J., Anderson, J. P., Tsao, P. S., Lenardo, M. J., Ashley, E. A., and Quertermous, T. (2008) Apelin signaling antagonizes Ang II effects in mouse models of atherosclerosis. *J. Clin. Invest.* **118**, 3343–3354
27. Hashimoto, T., Kihara, M., Imai, N., Yoshida, S., Shimoyamada, H., Yasuzaki, H., Ishida, J., Toya, Y., Kiuchi, Y., Hirawa, N., Tamura, K., Yazawa, T., Kitamura, H., Fukamizu, A., and Umemura, S. (2007) Requirement of apelin-apelin receptor system for oxidative stress-linked atherosclerosis. *Am. J. Pathol.* **171**, 1705–1712
28. Chandra, S. M., Razavi, H., Kim, J., Agrawal, R., Kundu, R. K., de Jesus Perez, V., Zamanian, R. T., Quertermous, T., and Chun, H. J. (2011) Disruption of the apelin-APJ system worsens hypoxia-induced pulmonary hypertension. *Arterioscler. Thromb. Vasc. Biol.* **31**, 814–820
29. Castan-Laurell, I., Dray, C., Knauf, C., Kunduzova, O., and Valet, P. (2012) Apelin, a promising target for type 2 diabetes treatment? *Trends Endocrinol. Metab.* **23**, 234–241
30. Lu, Q., Feng, J., and Jiang, Y. R. (2013) The role of apelin in the retina of diabetic rats. *PLoS One* **8**, e69703
31. Zhao, T., Lu, Q., Tao, Y., Liang, X. Y., Wang, K., and Jiang, Y. R. (2011) Effects of apelin and vascular endothelial growth factor on central retinal vein occlusion in monkey eyes intravitreally injected with bevacizumab: a preliminary study. *Mol. Vis.* **17**, 1044–1055
32. Tao, Y., Lu, Q., Jiang, Y. R., Qian, J., Wang, J. Y., Gao, L., and Jonas, J. B. (2010) Apelin in plasma and vitreous and in fibrovascular retinal membranes of patients with proliferative diabetic retinopathy. *Invest. Ophthalmol. Vis. Sci.* **51**, 4237–4242
33. Audigier, Y., Picault, F. X., Chaves-Almagro, C., and Masri, B. (2013) G protein-coupled receptors in cancer: biochemical interactions and drug design. *Prog. Mol. Biol. Transl. Sci.* **115**, 143–173
34. Sorli, S. C., Le Gonidec, S., Knibiehler, B., and Audigier, Y. (2007) Apelin is a potent activator of tumour neoangiogenesis. *Oncogene* **26**, 7692–7699
35. Heo, K., Kim, Y. H., Sung, H. J., Li, H. Y., Yoo, C. W., Kim, J. Y., Park, J. Y., Lee, U. L., Nam, B. H., Kim, E. O., Kim, S. Y., Lee, S. H., Park, J. B., and Choi, S. W. (2012) Hypoxia-induced up-regulation of apelin is associated with a poor prognosis in oral squamous cell carcinoma patients. *Oral Oncol.* **48**, 500–506
36. Kälin, R. E., Kretz, M. P., Meyer, A. M., Kispert, A., Heppner, F. L., and Brändli, A. W. (2007) Paracrine and autocrine mechanisms of apelin signaling govern embryonic and tumor angiogenesis. *Dev. Biol.* **305**, 599–614
37. Picault, F. X., Chaves-Almagro, C., Projetti, F., Prats, H., Masri, B., and Audigier, Y. (2014) Tumour co-expression of apelin and its receptor is the basis of an autocrine loop involved in the growth of colon adenocarcinomas. *Eur. J. Cancer* **50**, 663–674
38. Berta, J., Kenessey, I., Dobos, J., Tovari, J., Klepetko, W., Jan Ankersmit, H., Hegedus, B., Renyi-Vamos, F., Varga, J., Lorincz, Z., Paku, S., Ostoros, G., Rozsas, A., Timar, J., and Dome, B. (2010) Apelin expression in human non-small cell lung cancer: role in angiogenesis and prognosis. *J. Thorac. Oncol.* **5**, 1120–1129
39. Lacquaniti, A., Altavilla, G., Picone, A., Donato, V., Chirico, V., Mondello, P., Aloisi, C., Marabello, G., Loddo, S., Buemi, A., Lorenzano, G., and Buemi, M. (2015) Apelin beyond kidney failure and hyponatremia: a useful biomarker for cancer disease progression evaluation. *Clin. Exp. Med.* **15**, 97–105
40. Sorli, S. C., van den Berghe, L., Masri, B., Knibiehler, B., and Audigier, Y. (2006) Therapeutic potential of interfering with apelin signalling. *Drug Discov. Today* **11**, 1100–1106
41. Berta, J., Hoda, M. A., Laszlo, V., Rozsas, A., Garay, T., Torok, S., Grusch, M., Berger, W., Paku, S., Renyi-Vamos, F., Masri, B., Tovari, J., Groger, M., Klepetko, W., Hegedus, B., and Dome, B. (2014) Apelin promotes lymphangiogenesis and lymph node metastasis. *Oncotarget* **5**, 4426–4437
42. Macaluso, N. J., Pitkin, S. L., Maguire, J. J., Davenport, A. P., and Glen, R. C. (2011) Discovery of a competitive apelin receptor (APJ) antagonist. *ChemMedChem* **6**, 1017–1023
43. Zhou, N., Fang, J., Acheampong, E., Mukhtar, M., and Pomerantz, R. J. (2003) Binding of ALX40-4C to APJ, a CNS-based receptor, inhibits its utilization as a co-receptor by HIV-1. *Virology* **312**, 196–203
44. Masri, B., Salahpour, A., Didriksen, M., Ghisi, V., Beaulieu, J. M., Gainetdinov, R. R., and Caron, M. G. (2008) Antagonism of dopamine D2 receptor/beta-arrestin 2 interaction is a common property of clinically effective antipsychotics. *Proc. Natl. Acad. Sci. USA* **105**, 13656–13661
45. Evron, T., Peterson, S. M., Urs, N. M., Bai, Y., Rochelle, L. K., Caron, M. G., and Barak, L. S. (2014) G protein and β-arrestin signaling bias at the ghrelin receptor. *J. Biol. Chem.* **289**, 33442–33455
46. Hosoya, M., Kawamata, Y., Fukusumi, S., Fujii, R., Habata, Y., Hinuma, S., Kitada, C., Honda, S., Kurokawa, T., Onda, H., Nishimura, O., and Fujino, M. (2000) Molecular and functional characteristics of APJ. Tissue distribution of mRNA and interaction with the endogenous ligand apelin. *J. Biol. Chem.* **275**, 21061–21067
47. Huang, X. P., Mangano, T., Hufeisen, S., Setola, V., and Roth, B. L. (2010) Identification of human ether-à-go-go related gene modulators by three screening platforms in an academic drug-discovery setting. *Assay Drug Dev. Technol.* **8**, 727–742
48. Lee, D. K., Saldivia, V. R., Nguyen, T., Cheng, R., George, S. R., and O'Dowd, B. F. (2005) Modification of the terminal residue of apelin-13 antagonizes its hypotensive action. *Endocrinology* **146**, 231–236
49. Arrieta, O., Guevara, P., Reyes, S., Ortiz, A., Rembao, D., and Sotelo, J. (1998) Protamine inhibits angiogenesis and growth of C6 rat glioma; a synergistic effect when combined with carmustine. *Eur. J. Cancer* **34**, 2101–2106
50. Taylor, S., and Folkman, J. (1982) Protamine is an inhibitor of angiogenesis. *Nature* **297**, 307–312
51. Tiani, C., Garcia-Pras, E., Mejias, M., de Gottardi, A., Berzigotti, A., Bosch, J., and Fernandez, M. (2009) Apelin signaling modulates splanchnic angiogenesis and portosystemic collateral vessel formation in rats with portal hypertension. *J. Hepatol.* **50**, 296–305
52. Huang, J. S., Nishimura, J., Huang, S. S., and Deuel, T. F. (1984) Protamine inhibits platelet derived growth factor receptor activity but not epidermal growth factor activity. *J. Cell. Biochem.* **26**, 205–220
53. Neufeld, G., and Gospodarowicz, D. (1987) Protamine sulfate inhibits mitogenic activities of the extracellular matrix and fibroblast growth factor, but potentiates that of epidermal growth factor. *J. Cell. Physiol.* **132**, 287–294
54. Hughes, L. E. (1964) Treatment of malignant disease with protamine sulphate. *Lancet* **1**, 408–409
55. Casanovas, O., Hicklin, D. J., Bergers, G., and Hanahan, D. (2005) Drug resistance by evasion of antiangiogenic targeting of VEGF signaling in late-stage pancreatic islet tumors. *Cancer Cell* **8**, 299–309
56. Yang, J. C., Haworth, L., Sherry, R. M., Hwu, P., Schwartzentruber, D. J., Topalian, S. L., Steinberg, S. M., Chen, H. X., and Rosenberg, S. A. (2003) A randomized trial of bevacizumab, an anti-vascular endothelial growth factor antibody, for metastatic renal cancer. *N. Engl. J. Med.* **349**, 427–434
57. Alastalo, T. P., Li, M., Perez, Vde. J., Pham, D., Sawada, H., Wang, J. K., Koskenvuo, M., Wang, L., Freeman, B. A., Chang, H. Y., and Rabinovitch, M. (2011) Disruption of PPARγ/β-catenin-mediated regulation of apelin impairs BMP-induced mouse and human pulmonary arterial EC survival. *J. Clin. Invest.* **121**, 3735–3746

Received for publication September 27, 2016.
Accepted for publication February 7, 2017.